CleanAtlantic

Tackling Marine Litter in the Atlantic Area

WP 5: Monitoring and Data Management
DELIVERABLE 5.2. – Monitoring the presence of marine litter in the marine environment

Interreg Atlantic Area
European Regional Development Fund
EUROPEAN UNION
Clean Atlantic

WP	WP5
ACTION	2
LAST UPDATED	30/04/2019
VERSION	1
AUTHORS	LENKA FRONKOVA - CEFAS
PARTICIPANTS	

Cefas Document Control

Submitted to:	Clean Atlantic
Date submitted:	23/10/2019
Project Manager:	Jacky Read
Report compiled by:	Lenka Fronkova
Quality control by:	Thomas Maes/ Josie Russell
Approved by and date:	
Version:	2
Recommended citation for this report:	

Index

Development and improvement of monitoring methods for marine litter

1. Introduction

Importance

Due to a rapid production of plastics since 1950s, there is an increasing concern about global pollution of plastic debris in the open oceans (Cózar et al., 2014). Around 60-64% of the terrestrial load of plastic to the sea is estimated to be transported to open-ocean waters, with the greatest concentration of floating debris being modelled in the subtropical ocean gyres (Maximenko, Hafner and Niiler, 2012; Lebreton, Greer and Borrero, 2012). In these areas, a high concentration of floating litter is visible using remote sensing. This was confirmed by a survey in the Great Pacific Garbage Patch which shows that polyethylene (PE) and polypropylene (PP) are the most common floating polymers (Lebreton et al., 2018). Despite floating plastics being visible on the sea surface, there is still a mis-match between the hydrocarbon load to the oceans and the amount of plastics found in the coastal areas and on the sea surface. As such, it is estimated that there are sinks of plastic debris on the ocean floor. Similarly, this mis-match is caused by plastic debris being fragmented into particles <2.5 cm, commonly known as microplastics. Microplastics can be ingested by a wide range of organisms, from small fish to large mammals and birds (Boerger et al., 2010; Choy and Drazen, 2013; de Stephanis et al., 2013). There are various mechanical effects of plastics, for example gastrointestinal obstructions in seabirds (Azzarello and Van-Vleets, 1987) but also accumulation of chemical contaminants from plastics and sea water in the receiving organisms which can cause death (Teuten et al., 2009). Marine litter can also cause serious economic damage as losses for coastal communities, tourism, shipping and fishing. Fishing industry could equal to almost €60 million which is 1% of total revenues of the EU fishing fleet in 2010 (EU Commission, 2018) Due spatial and temporal variability of marine litter to threats plastics impose on environment and, it is important to develop effective methods for their frequent, repetitive and large scale monitoring in order to facilitate any cleaning activities and to better understand and map plastic hotpots. Estimating litter trends over time is needed for efficient monitoring programs, management and reduction measures (Galangi, Hanke and Maes, 2015). Several regional and global initiatives were launched such as OSPAR Regional Action Plan, G7/G20 Marine Litter Action Plan or UN Sustainable Development Goals which aim for an international litter management program (Maes, 2017). Pollution of the seas from plastics and microplastics is one the three major areas of the Strategy for Plastics that was adopted in January 2018 by European Union Commission (EU Commission, 2018). Therefore, developing and improving methods of plastic litter hotspots identification will lead to improved litter management systems in the east Atlantic region and potentially worldwide.

2. Literature Review

In the past five years, there has been numerous remote sensing techniques successfully utilised to map marine litter. Examples of these are using unmanned aerial vehicles (UAVs), cameras manned at the coast/beaches that can collect high resolution data for repeatable monitoring. Methods such as image classification or machine learning can yield successful results in automatic identification of litter targets and their classification. Although these methods prove to be successful, they do not provide an option for monitoring larger spatial scales. Aircraft surveys compensate fort this limitation of UAVs or fixed cameras, however, they are rather expensive, therefore cannot be used for repetitive monitoring. Freely available satellite data products from Copernicus or NASA have become a focus of research on identification of large spatial scale of plastic litter hotspots only recently. As Maximenko et al. (2016) and Moller et al. (2016) point out remote sensing imagery with moderate to high temporal, spectral and spatial resolution would enable explore distribution of floating marine plastic debris. In addition, Asner (2016) argues that spectroscopy does not require a high spectral or spatial resolution but a spectral library of marine debris which can be used to detect them remotely. Garaba and Dierssen (2018) show that marine harvested dry and wet macro/micro plastics have notable absorption dips at ~931, 1214, 1417 and 1732 nm which were tested in laboratory conditions using spectroradiometer (Figure 1). However, only 1214 and 1732 plastic absorption features were observed through atmosphere column. This can be explained by water absorption around 950 and 1400 nm wavelengths. Therefore 1215 and 1723 were used to calculate hydrocarbon index which maps out hydrocarbons in hyperspectral AVIRIS imagery in a landfill (Garaba and Dierssen, 2018). Similarly, Martinez-Vincent et al. (2019) found out that multispectral data centred around 1732 nm is enough for a successful identification of litter on a sandy beach. Other authors such as Asner 2016 or Murphy et al. 2018 also prove that there are specific bands around NIR and SWIR where plastics have unique spectral signatures.

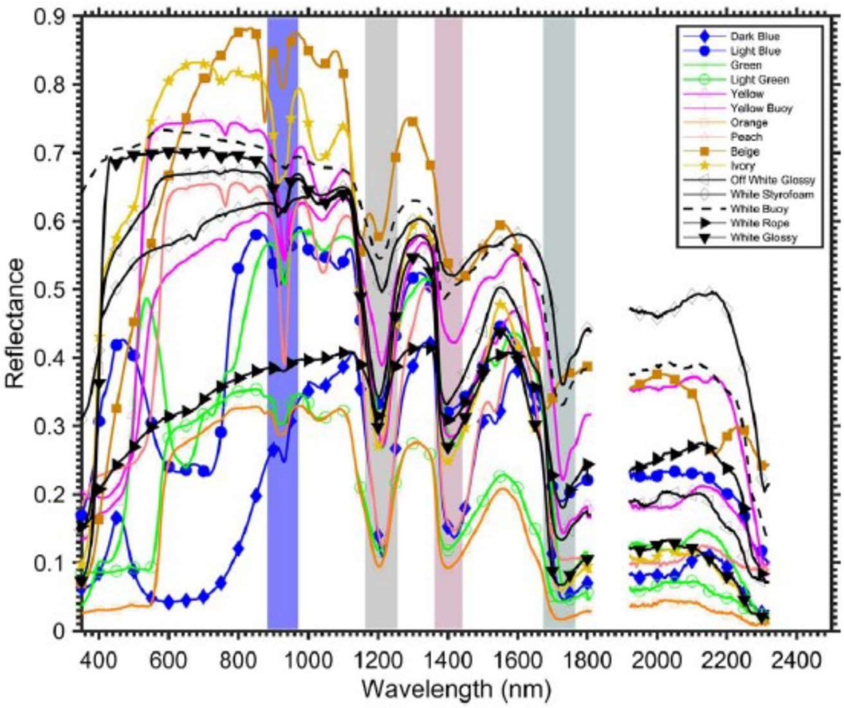

Figure 1. Spectral signatures of harvested marine plastic debris (Garaba and Dierssen, 2018).

Despite laboratory experiments showing unique spectral signatures of plastics, detecting them using satellite data can be problematic. Preliminary results from Plastic Litter Project conducted in 2018 by the University of the Aegean show that the spectral signature of the plastics detected in Sentinel-2 pixels for clear plastic bottles, fishing nets and blue plastic bags vary depending on the percentage of the material covering the pixel. In other words, the bulk spectral signature of the pixel present in Sentinel-2 imagery is influenced by the background surface. Figure 1 shows plastics that covered at least ~34% of the pixel's area undergo an increase in spectral reflectance in B08- 842 nm central wavelength and a significant absorption dip in B09-945nm. This is especially apparent for plastic bottles, with a weaker pattern for plastic bags and fishing nets which require at least 50% of pixel coverage to be detected (Topouzelis and Papakonstantinou, 2019). This can be explained by the radiative transfer balances of the radiation through thin plastic such as bags or nets. Overall Topouzelis and Papakonstantinou (2019) argue that Sentinel 2 data can be used to detect areas where the plastics covers at least half of the pixel spatial resolution and the marine plastics is observable from space even if submerged in the water.

All these studies (summary Table 1) show that it is possible to detect high concentration of plastic marine litter from space using specific spectral signatures tested in laboratories and satellite data. However, none of the studies compared spectral signatures of macro-plastics to different cover types both across space and time. This is important to research in order to determine the range of macro-plastic spectral reflectance obtained from satellite data and its variation across time. This range can be compared to ranges of other cover types such as deep/shallow water, beaches, urban areas or vegetation to investigate whether it is possible to differentiate among different cover types and use this knowledge to create a method that automatically detects plastic litter hotspots. As such this, project determines spectral ranges of different cover types across time and assess whether it is possible to use the ranges in automatic litter identification. Furthermore, this study compares commercial high spatial resolution data from WV3 to freely available but coarser Sentinel data. The following are the specific aims the project is going to address.

Aims of this project

The objectives of this project are to analyse, develop and improve monitoring methods of marine litter. In order to do that the following objectives are going to be answered:

1. Assess feasibility of Sentinel 2 data in identifying plastic litter hotspots.
2. What are the spectral ranges of polymers using Sentinel 2 data?
3. Developing a method of plastic litter hotspots identification.

Table 1. Summary of the literature review on plastic litter using remote sensing.

Author	Findings
Topouzelis and Papakonstantinou, 2019	• Reflectance of polymers peaks in 842 nm (Sentinel 2 data) • Macro-plastics is detectable from space if at least half of the pixels are covered by plastics
Martinez-Vincent et al. 2019	• Multispectral data around specific wavelengths are enough to detect plastic litter • Reflectance peaks around 1732 nm
Garaba and Dierssen 2018	• Absorption band depths of dry and wet macro/micro plastics at 1215 and 1732 nm (resemblance of raw polymers PP, LDPE, PET) • Hydrocarbon index- AVIRIS (landfill) • Problems with ground-truthing
Murphy et al. 2018	• model to detect floating debris (optical and geometric properties) • single (750nm) or dual (NIR and SWIR) band algorithm
Asner, 2016	• spectroscopy of polymers- does not require a high spatial resolution if spectral resolution is high- suggests • spectral library of marine debris is needed
Guardado, 2015	• Spectral fingerprints of 12 Plastic Resin Groups (SWIR &MIR)- multispectral library
Moroni et al, 2015	• PET and PVC absorption peaks (~1200 nm and ~1600nm)

Figure 2. Reflectance of different plastic objects using Sentinel 2 data (Topouzelis and Papakonstantinou, 2019).

3. Methodology

In order to answer the objectives, set in section 2.1., the following methodology was used:

1. Identify study areas where plastic objects are static and at least 10 x 10 m wide. This needs to be done to ensure the certainty that the plastic objects that are observable from satellite images are polymers without ground-truthing (conducting a survey). Also, 10 x 10 m is the highest resolution from Sentinel 2, therefore the study areas need to depict large plastic objects.
2. Download a timeseries of Sentinel 2 data. Ideally the time resolution was monthly, however, in case the cloud cover obstructed the view less frequent data was obtained. At least 12 data points were downloaded per study area to show a yearly variation.
3. Apply atmospheric correction to convert top of the atmosphere reflectance (TAP) to bottom of the atmosphere (BOT) using Sen2Core library.
4. Resample data to the same resolution (10 x 10 m), clip to a smaller study area.
5. Identify surface cover objects using True colour (RGB), false composites and NDVI (Normalized Difference Vegetation Index).
6. Calculate average spectral reflectance, NDVI and NDBI (Normalized Difference Build Index) of each object (Zonal Statistics in ArcGIS 10.5 version) across the timeseries and plot these.
7. Determine the spectral ranges of each surface cover type.
8. Use these ranges in automatic identification of macro-plastics.

4. Study areas

According to point 1 in Methodology section 3, three study areas were identified:

Eden

Eden Project was constructed in a former dredging area. Hexagonal pentagon domes were built made of tetrafluoroethylene copolymer (ETFE) material. ETFE is also so called ‘cling film with attitude’ since it transmits UV radiations, is non-stick, self- cleaning and lasts for more than 25 years. (Eden, 2019) (Figure 3)

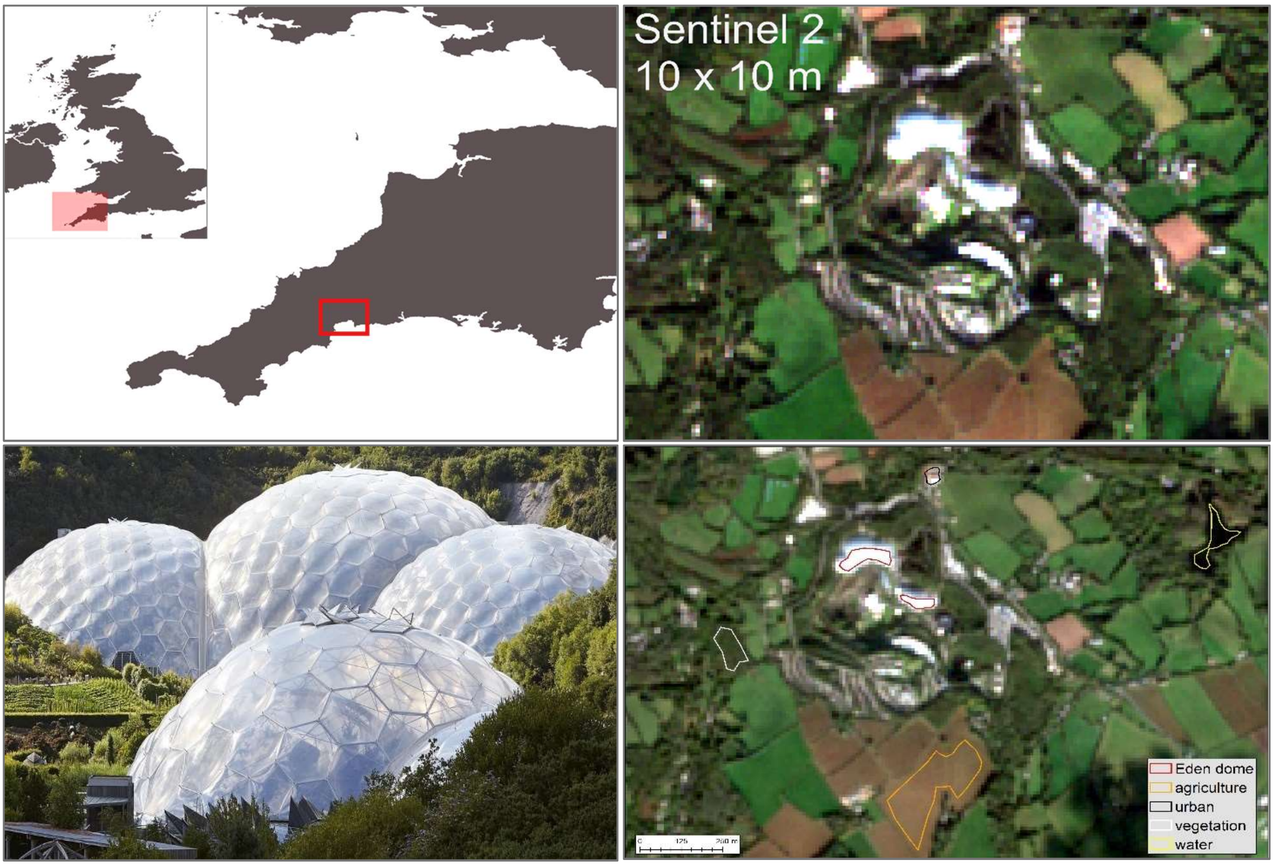

Figure 3. Eden project case study.

Thilafushi

This so-called Litter Island in Maldives is an artificial island where most of the litter is accumulated from other surrounding islands in the Maldives archipelago. Recently, some boatmen have dumped rubbish into the surrounding lagoons due to a long waiting time to unload the litter and there are threats of litter falling into the sea (BBC, 2011). The main part of the landfill is around 200 x 200 m big and it has a continuous litter cover (Figures 4).

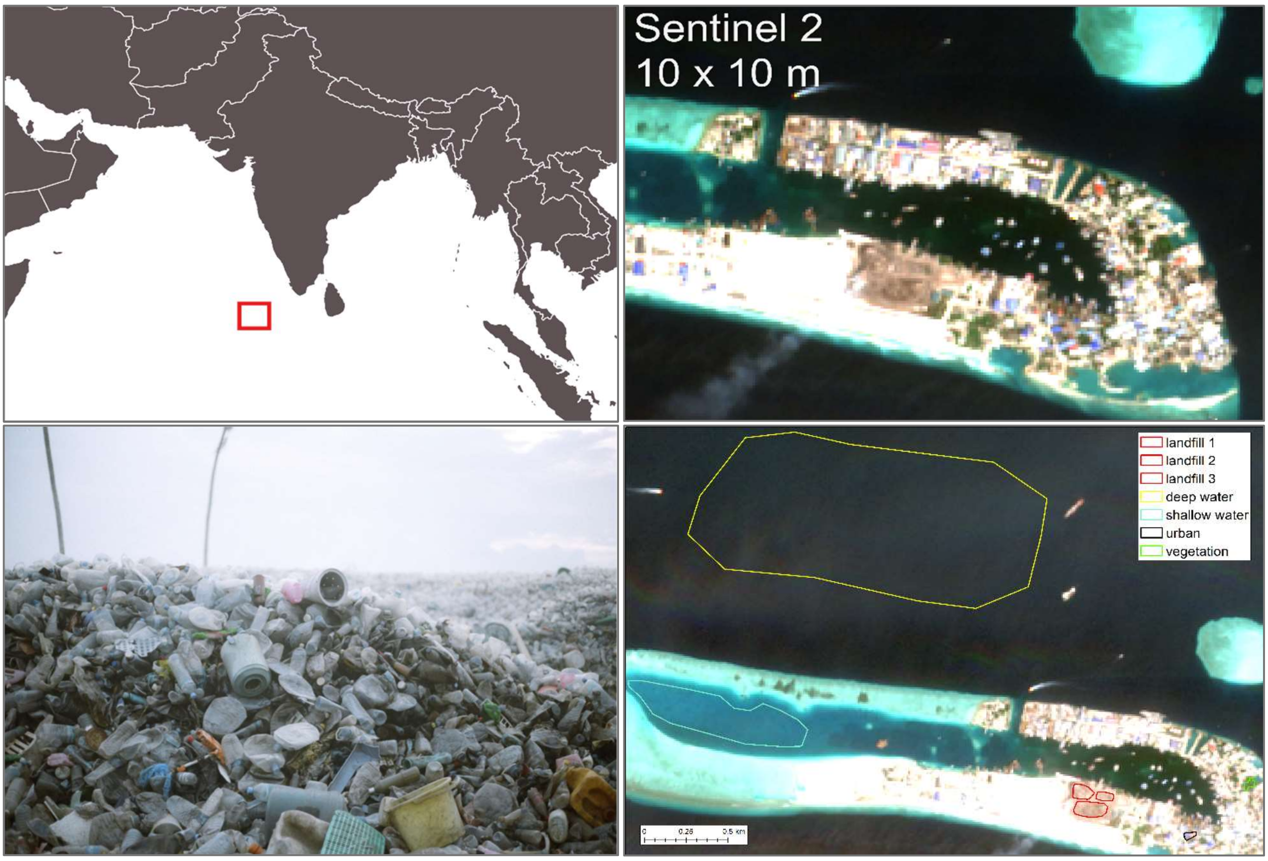

Figure 4. Thilafushi case study.

Mytilene

Plastic Litter Project conducted in 2018 by the University of the Aegean on 07/06/2018 composed of placing 10x10m plastic objects- fishing nets, bags and bottles on the sea surface. Sentinel 1, 2, UAVs and other commercial satellites were used to identify these objects from the sea surface. (Marine Remote Sensing Group, 2019) (Figure 5).

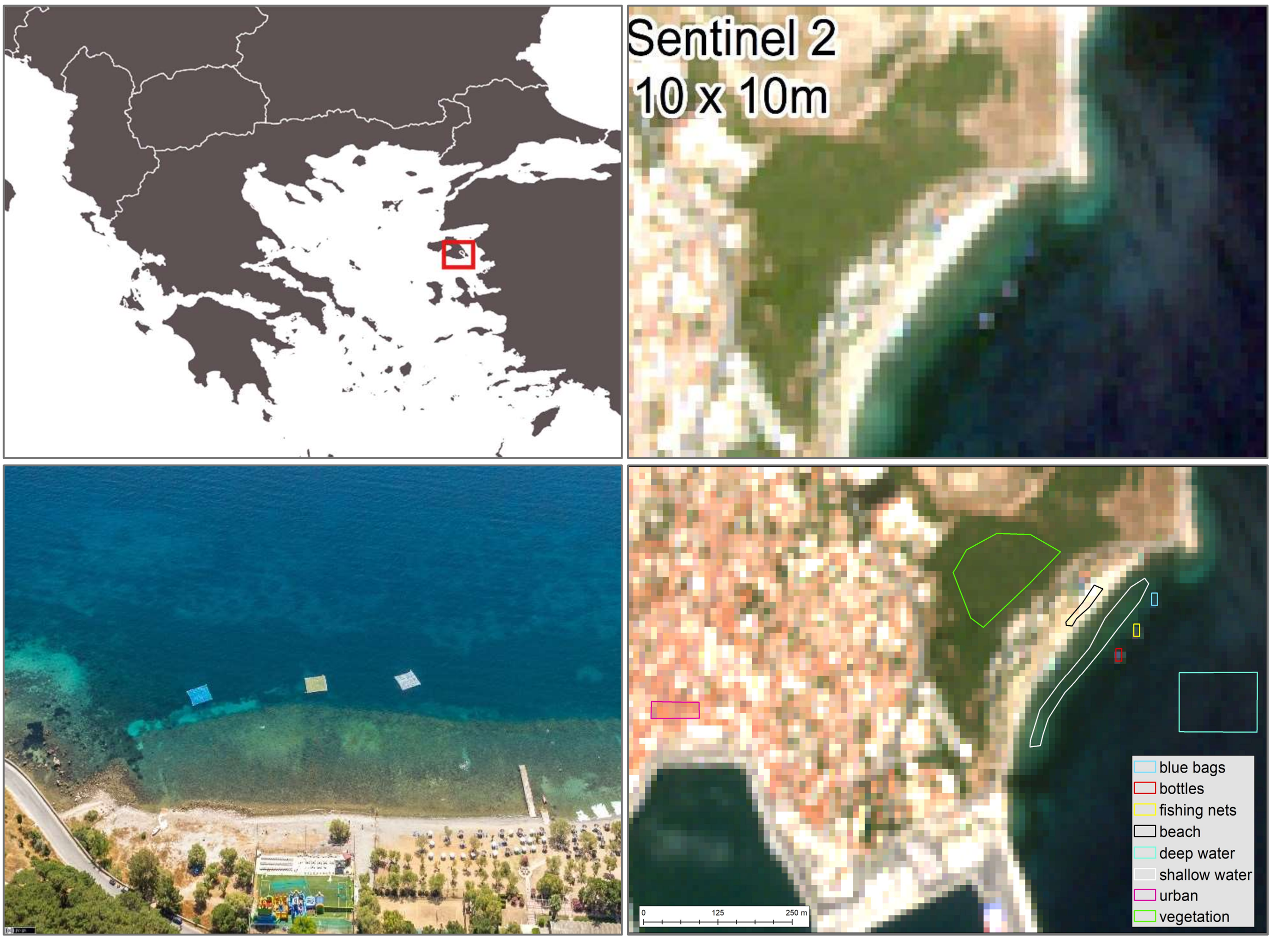

Figure 5. Mytilene case study.

5. Results

Spectral Reflectance

5.1.1. Plastic litter on land

Synthetic hydrocarbon objects in Eden and Mytilene study areas show an overall increase in reflectance between 740-865 nm in near-infrared wavelength (Figures 6 - 9). These correspond to Sentinel 2 B06- 740 nm, B07- 783 nm, B08- 842 nm and B08A- 865 nm central wavelengths. The reflectance peaks in B08 – 842 nm with a sharp absorption drop in B09- 945 nm central wavelength. A considerable variation in reflectance is expected in vegetation as it changes seasonally and to a lower degree for urban areas- which is shown in Figure 6 and Appendix 1. Since Eden domes are static polymer objects they should not change seasonally, and a low variation in reflectance was expected. Dates 19/12/2017 and 30/10/2018, however, depict a much higher reflectance than the rest of the data points. The reason for this fluctuation is unknown. Appendix 1 shows minimum, maximum, mean, standard deviation and coefficient of variation for each surface cover type in Eden study area between April 2017 and January 2018. The lowest reflectance of plastic domes is in SWIR B12-2190 nm with the highest reflectance in B08 – 842 nm. Since B08 has almost twice bigger reflectance than B12, this project suggests using a difference between these two bands to map the presence of synthetic hydrocarbons. Bands B08 and B12 have very similar values for urban and water cover types, but as in case of polymers, reflectance in agriculture and vegetation surfaces in B08 and B12 is almost twice bigger. Therefore, for land mapping of plastic litter, firstly vegetation will be removed using NDVI > than 0.5, as this is the minimum NDVI for healthy vegetation in Eden case study (Appendix 2).

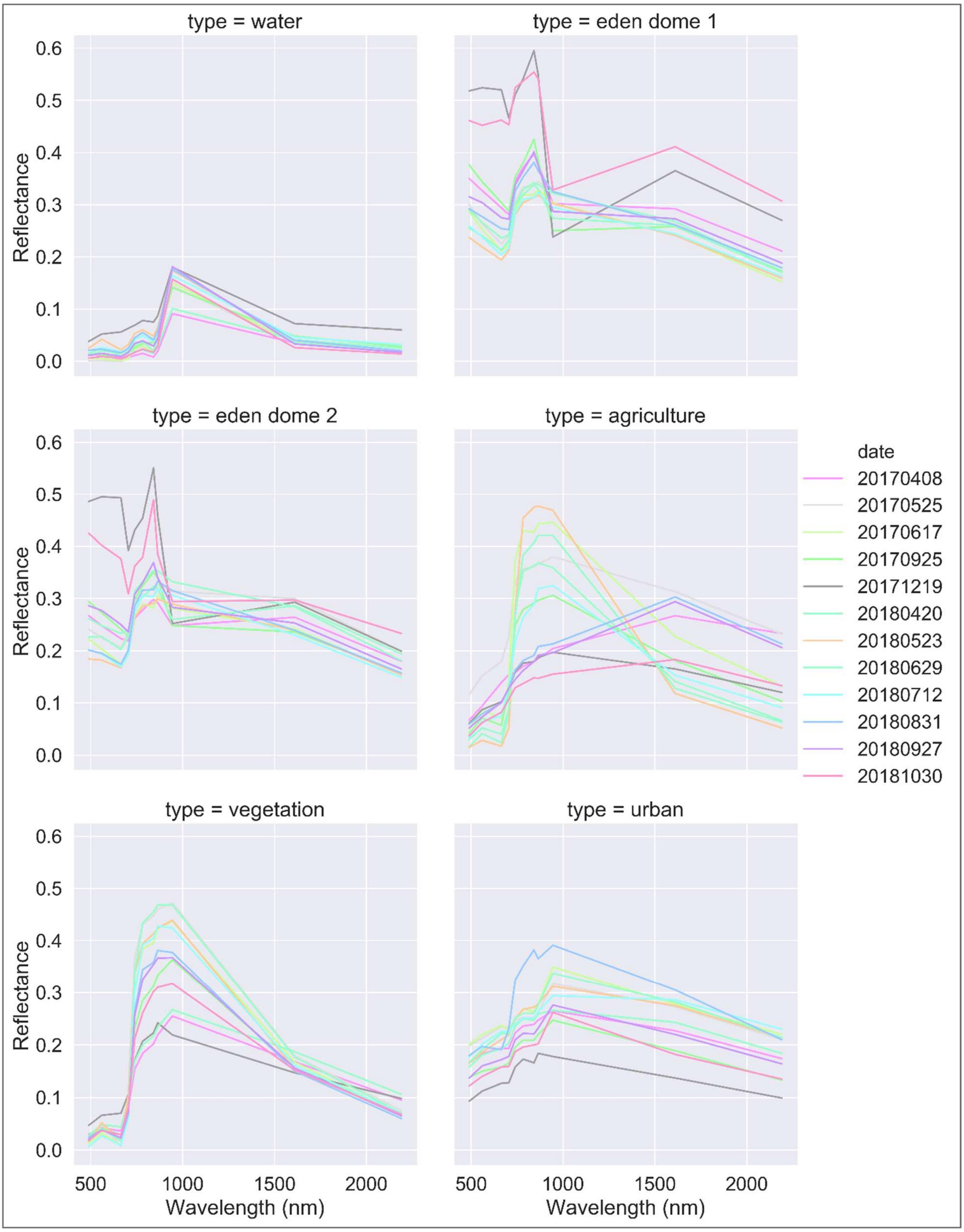

Figure 6. Spectral signature graphs for different cover types for Eden case study.

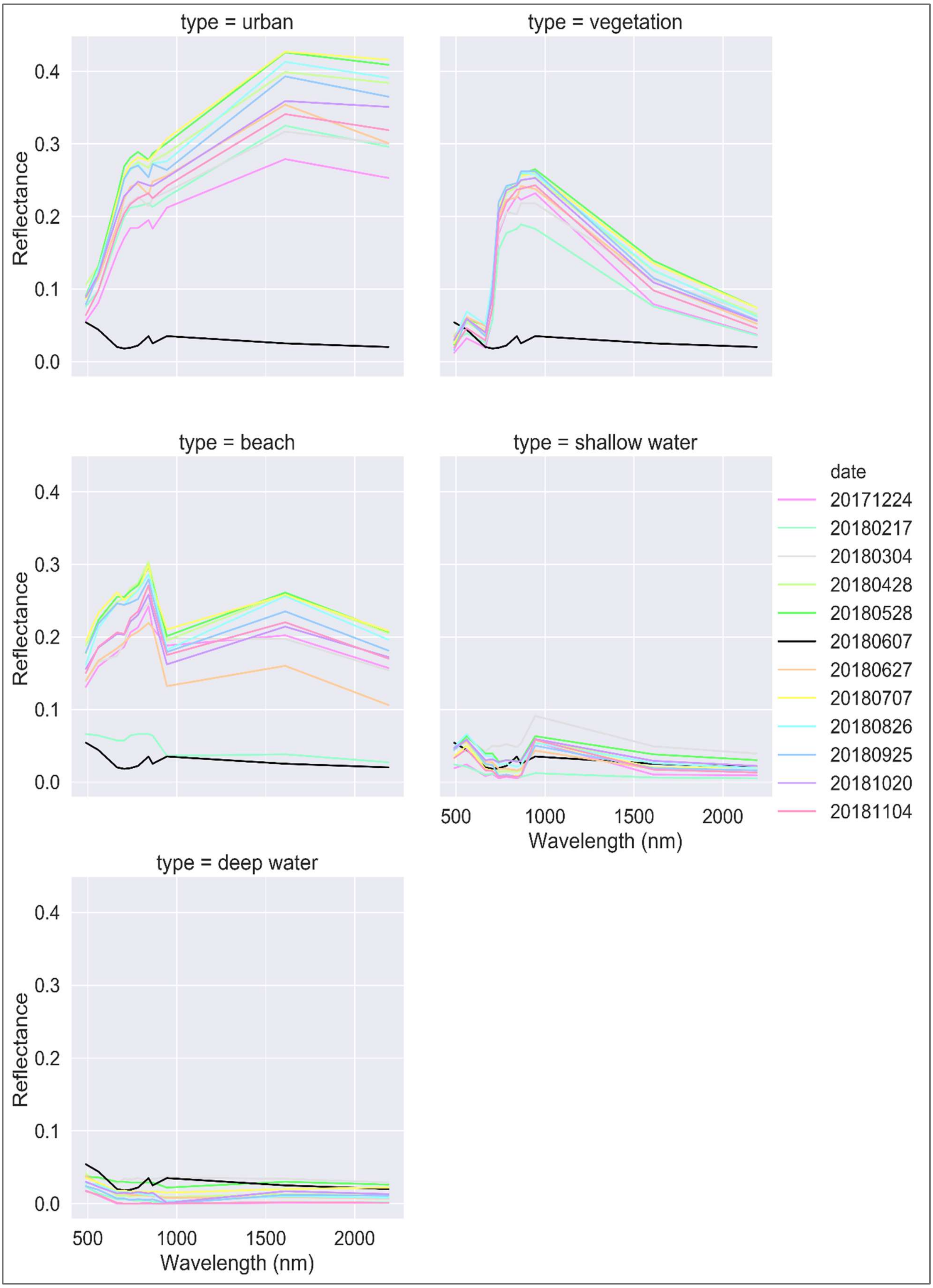

Figure 7. Spectral signature graphs for different cover types versus plastic bags.

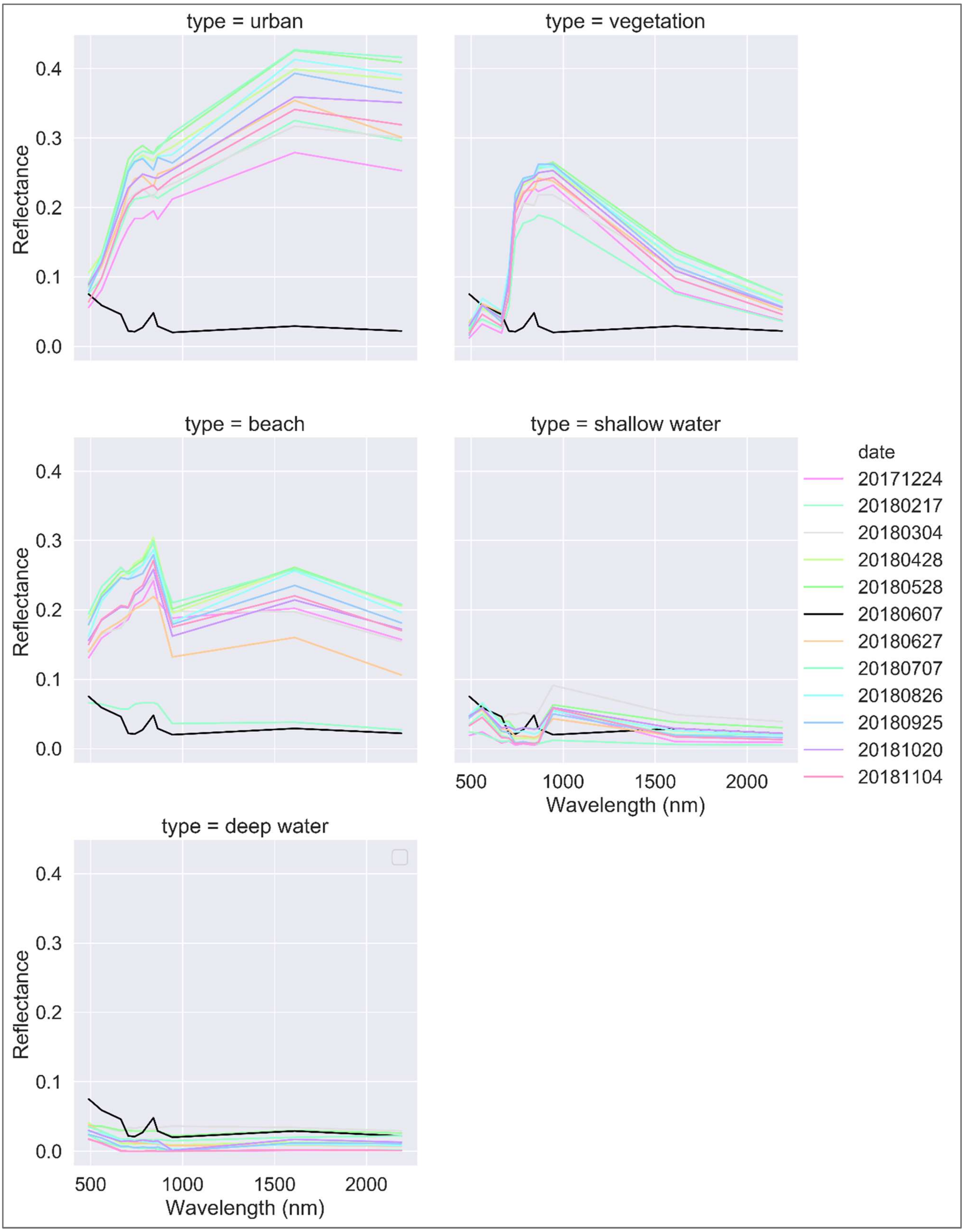

Figure 8. Spectral signature graphs for different cover types versus plastic bottles.

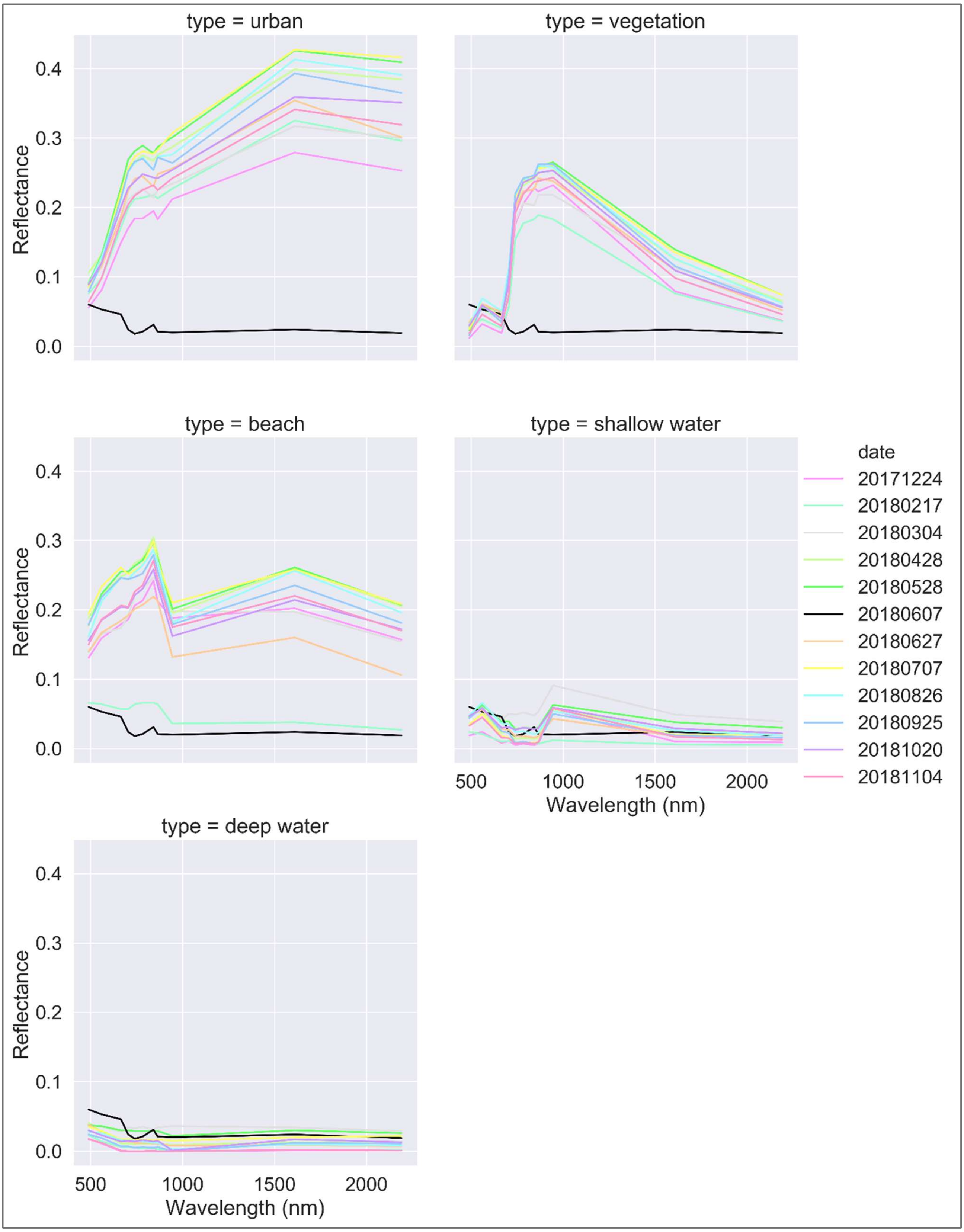

Figure 9. Spectral signature graphs for different cover types versus fishing nets.

5.1.2. Plastic litter on the sea

It was not possible to see the variations across time for plastic objects in Mytilene case study, since Sentinel 2 data where the plastic objects were detectable were available only for 06/07/2018, and after this date the objects were removed from the water surface. Despite it, this example is important as it provides an insight on the reflectance of plastics surrounded/submerged into water. The spectral reflectance graphs of plastic bags, bottles and fishing nets (Figure 7, 8, 9) show that these objects have very different shapes from urban, beach and vegetation cover types. This is not the case for plastics and water. Spectral reflectance of plastics coincides with shallow and deep-water reflectance, mainly in SWIR wavelengths, therefore floating plastic litter might be difficult to differentiate from water. Comparing reflectance of plastic bags, bottles and fishing nets (Figure 10), the spectral reflectance peaks in 842 nm (B08) and there and drop in reflectance by almost a half from 842 nm (B08) to 945 nm (B09). These drops in reflectance are present for plastic bags and nets too but they are not as pronounced as in case of bottles. This can be explained by plastic bags and nets being submerged into the water or different absorption properties of plastic types. Although B12 does not exhibit the lowest reflectance in Mytilene case study, B08 and B12 are going to be used to map plastic litter on the sea surface since it is not possible to draw conclusions on plastic reflectance from one instance in time. Therefore, Normalized Difference Index will be used to extract only water bodies from Sentinel 2 image and then B08-B12 difference will be applied and compared to NDBI.

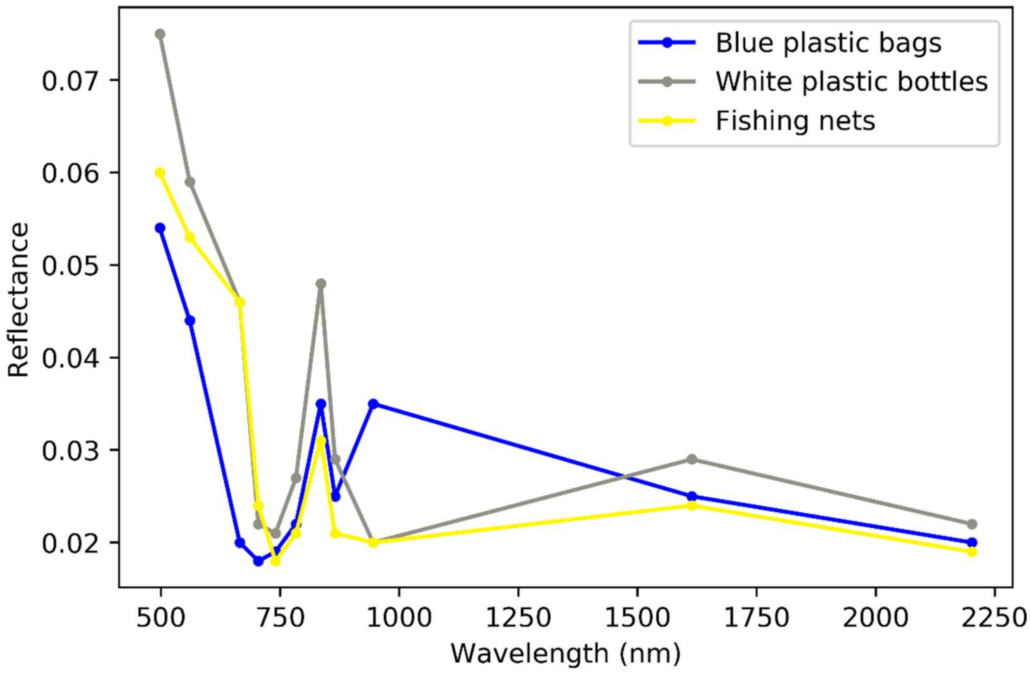

Figure 10. Average reflectance of plastic bottles, bags and nets in 2 pixels which represent these objects.

5.1.3. Mixed plastic litter

In real conditions, plastic litter will be diverse and mixed with other marine debris, which can result in high variation of reflectance. This is the case of Thilafushi landfill study area. Figure 11 shows that spectral reflectance graphs of three landfill objects do not rise considerably in B08, drop in B09 with a further decrease until B12 (SWIR) as it was present in Eden and Mytilene. In Thilafushi landfill, reflectance gradually increases and peaks in B11- 1610 nm central wavelength and then levels out/drops. There are no significant peaks or troughs. Although the spectral reflectance graphs are very different between landfill and deep/shallow waters, they overlap in NIR with vegetation and urban cover types. Although the mapping method of using B8/B12 difference is applied to Thilafushi landfill in order to compare the study areas, the landfill does not exhibit any clear reflectance pattern in these bands.

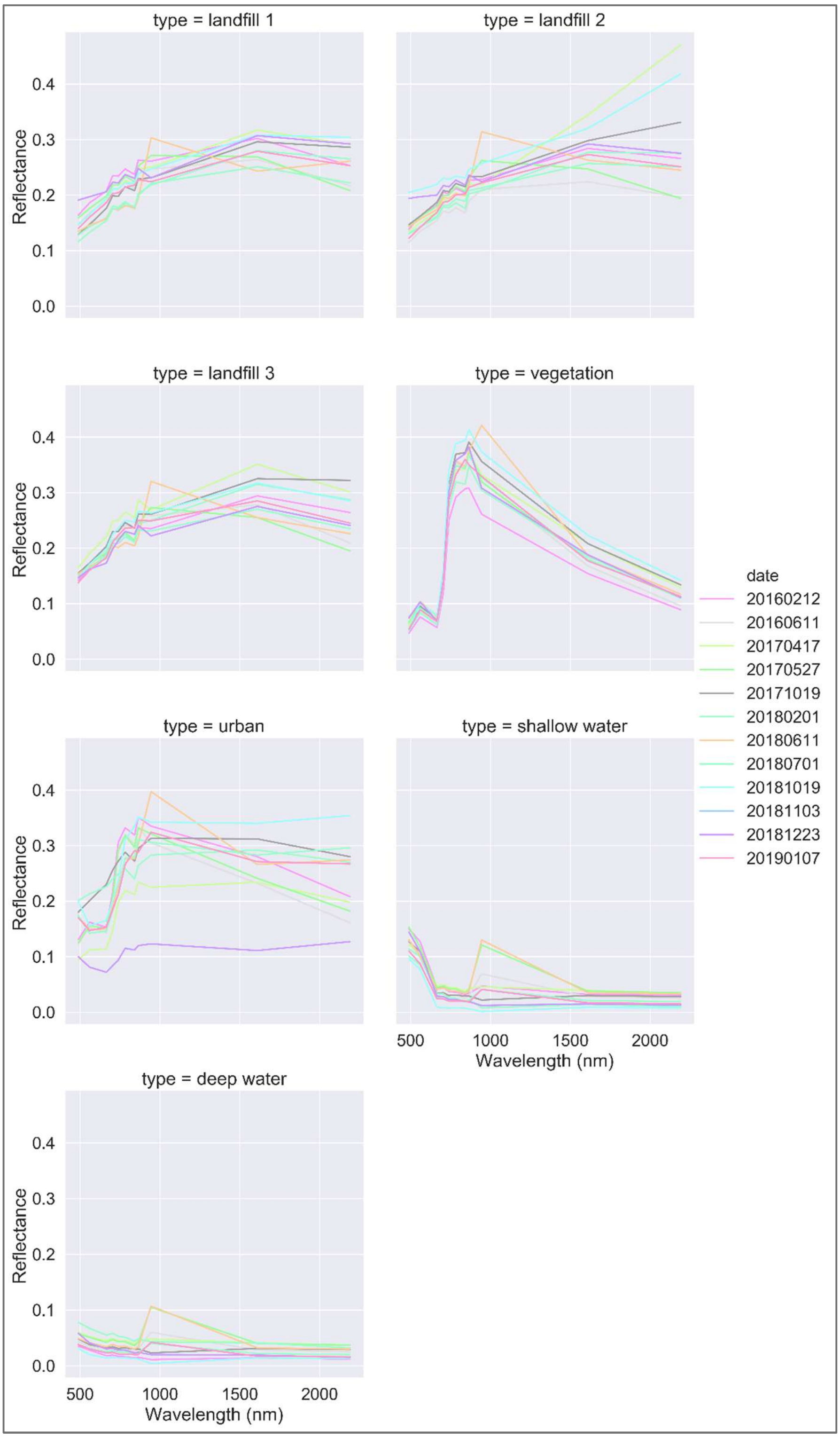

Figure 11. Spectral reflectance of different cover types for Thilfushi study area.

Mapping plastic litter hotspots

Using the information from the spectral graph signatures on a sharp difference between B08 and B12 reflectance for plastic litter, the following workflows are suggested for mapping plastic litter hotspots in areas on land and on the sea:

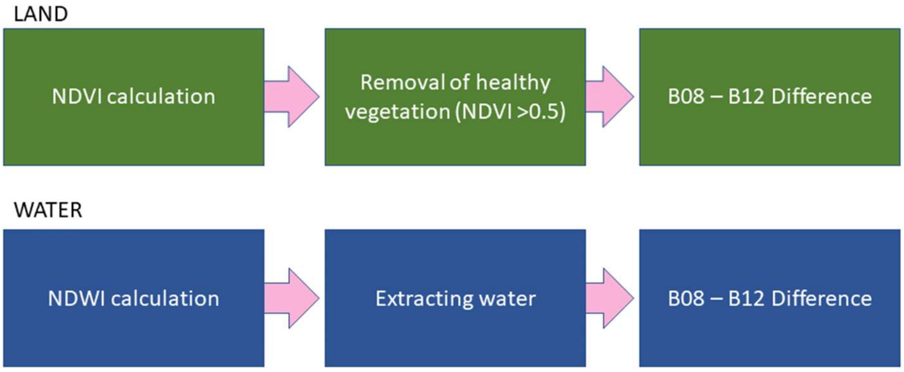

Figure 12 illustrates true colour (RGB), areas left after healthy vegetation was removed and the B08 – B12 differences in the remaining areas which are not classified as vegetation. The highest difference between bands B08 and B12 correspond to 2 domes that were digitised as plastic objects; hence this method can map out areas where the plastic objects cover substantial proportion of the Sentinel-2 pixels. This method also mapped out other objects which have high differences (orange circles). After conducting checks using google maps, these areas also appear to be synthetic hydrocarbons. However, fieldwork and ground-truthing still need to be conducted to confirm these.

Using the same method to map synthetic hydrocarbons on water, however, seems to be rather problematic. As Figure 13 depicts, waterbodies were identified using NDWI and B08 – B12 difference was calculated. The results show that the difference of the two wavelengths is high in the pixels that correspond to plastic bags, nets and bottles, meaning that these objects were mapped successfully. However, across the area, there are multiple other pixels which show high differences such as objects near the beach (Figure 14 A), spit of land (Figure 14 B) and a ship (Figure 14 C). This can cause problems in automatic mapping of litter on the sea surface. However, the nature of these objects can be easily verified using true colour images for the ship and spit of land. It becomes more problematic for the pixels near the beaches (Figure 14 A), where it is difficult to determine what the high difference pixels represent even using high resolution 1.2 x 1.2 m WV3 data.

The pattern that is observable in the Eden and Mytilene case study where B08-B12 difference can be used in an iterative process to classify pixels as plastics is not present in Thilafushi landfill. Since spectral signature graph (Figure 15) does not depict any clear pattern (pronounced peaks/troughs) this is also reflected in the B08 – B12 difference (Figure 9). In Figure 15, the high difference between the bands is in case of ships which was similar to Mytilene case study, but the landfill itself shows low differences between B08 and B12. Also, there are many other areas on the island itself which have high differences but are not synthetic hydrocarbons. This example shows that this method does not work when pixels are composed of diverse and mixed litter material. Also, it is not possible to determine what composition these landfills are without conducting fieldwork. As such, this method can distinguish areas of dense plastic objects, but it is not applicable in cases mixed litter.

Figure 12. Mapped plastics on land- Eden case study.

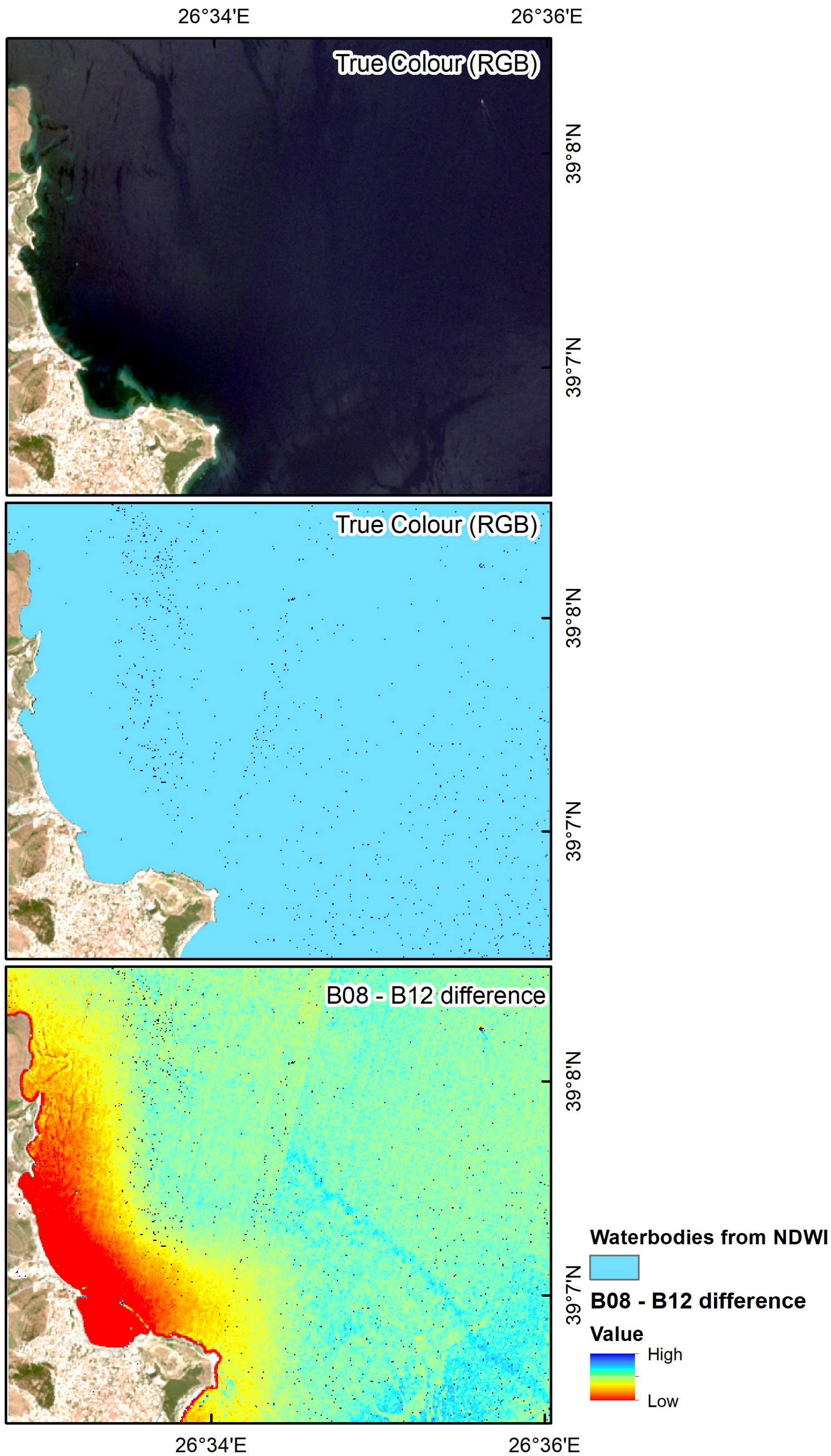

Figure 13. Mapped plastics on the sea surface- Mytilene case study.

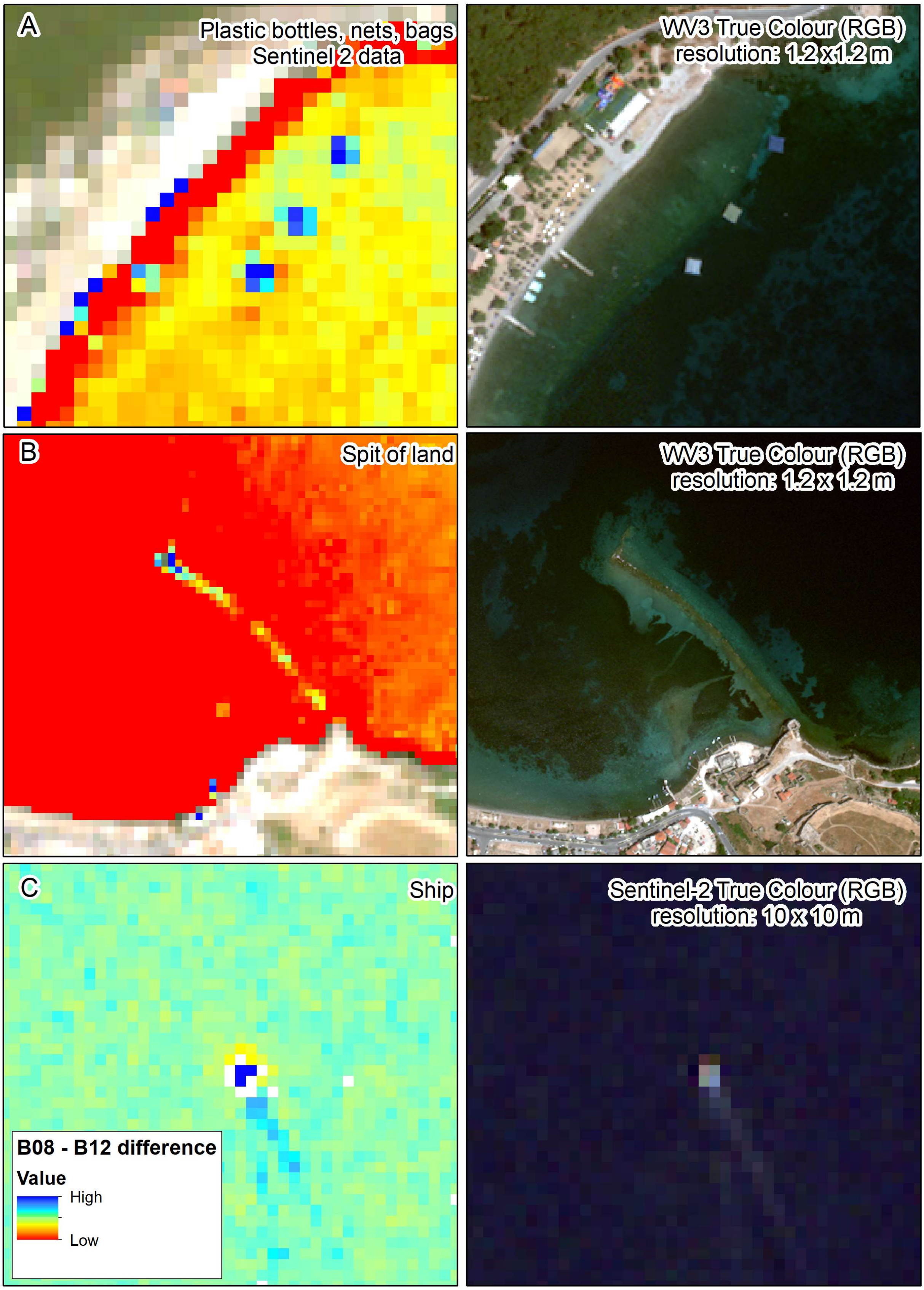

Figure 14. Objects which show the highest difference using B8/B12 wavebands on the sea surface.

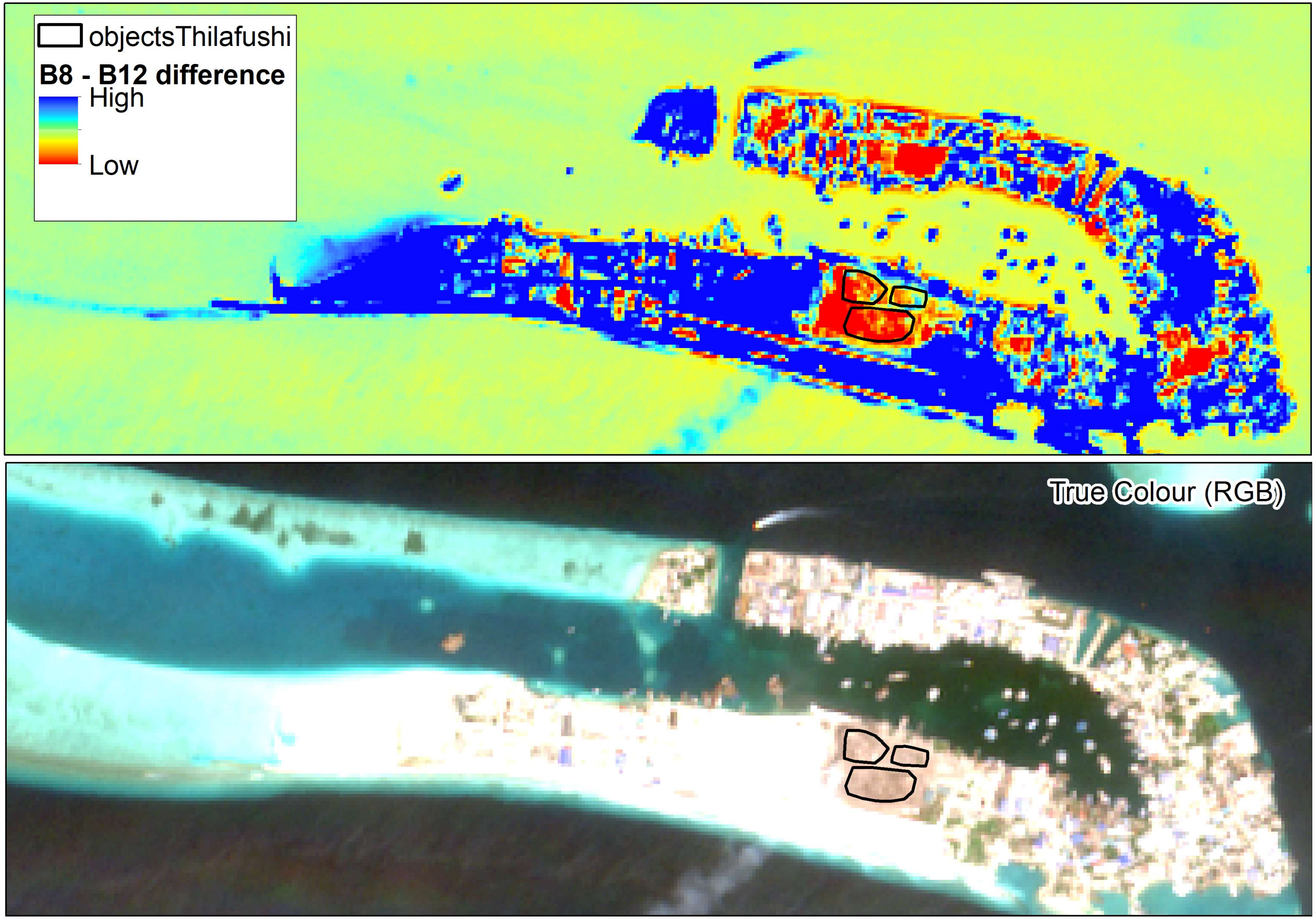

Figure 15. Mapped plastics using B8/B12 approach in Thilafushi case study.

6. Discussion

Overall, spectral signatures of plastic objects investigated in this project show the maximum reflectance in NIR 842 nm and the lowest reflectance in SWIR B12 2190 nm. Similarly, these objects depict a gradual increase in reflectance in the NIR with a sharp drop in band B9. Combined patterns from spectral graphs of Eden and Mytilene case studies are similar to reflectance graphs from Topouzelis and Papakonstantinou (2019). However, in case of this project emphasis was put on exploring spectral graphs of plastics across time and comparing them to other cover types, since it is difficult to draw conclusions on using reflectances from Sentinel-2 data from 1 point in time as it was in case of Topouzelis and Papakonstantinou (2019). As such, by looking at 25 monthly reflectance of plastic objects (24- Eden case study, 1 Mytilene), it is possible to argue that the pattern seen in the spectral graphs of plastic objects is not caused by chance.

Thilafushi case study shows very different spectral signatures of the landfill compared to Eden and Mytilene. This is most likely caused by diverse rubbish present (not only plastics) at the landfill which is impossible to identify without conducting a fieldwork. As Topouzelis and Papakonstantinou (2019) point out, the percentage of specific cover type constituting individual pixels in satellite data influence the overall bulk reflectance. Therefore, the more mixed and diverse the cover type is, the more varied the reflectance becomes. However, this does not seem to be the case for wavebands 1215 and 1732 nm that Garaba and Dierssen (2018) used to calculate hydrocarbon index of a landfill containing lots of polymers from hyperspectral data. Similarly, Martinez-Vincent et al. (2019) used 1732 nm to detect plastic objects on the beach. Sentinel 2 does not contain these specific wavebands, hence spectral graphs do not show any conclusive pattern for these cover types.

Using knowledge from spectral graphs of plastic litter, this project proposes workflows for automatic identification of litter based on Sentinel-2 data. Since, band 8 shows the peak and band 12 the trough, these two bands are utilised to compute a relative difference where the higher the difference, the more likely the pixel can be considered to contain plastics. This approach works for Eden case study, where not only the plastic domes show the highest difference, but also other objects which are believed to be plastics using verification from google maps. Ideally, this will be proved by visiting the site. Applying this method on the sea surface classifies plastic bottles, nets and bags, however, there are also false positives- pixels with high differences which are not plastics but ships or spit of land. These false positives can be ruled out using true colour images though. In terms of Thilafushi case study, this method does not successfully detect landfill at all which might be down to its mixed composition. As such, Sentinel 2 data can be used to detect plastic litter (objects) from space in an automatic way, but it fails when the composition of the pixels are not pure plastics. Although plastics account for almost 99.9% of floating debris, there can be other material together with biofouling which can change the spectral reflectance of individual pixels depending on what percentage of the pixel surface area they cover. Consequently, more fieldwork where cover type with more realistic conditions set-up will be (mixed debris with plant material) is needed to be conducted. This is especially important due to ground-truthing of remote sensing data.

7. Conclusion

This study assesses freely available Sentinel 2 data in terms of automatic identification of plastic litter hotspots. Both Eden and Mytilene case studies show specific patterns of spectral signature graphs, peaking at 842 nm (B8) with a sharp drop in 945 nm (B9) and the lowest reflectance at 2190 nm (B12). Thilafushi landfill did not show the same pattern due to mixed composition of litter. It is possible to use high differences between B8 and B12 to map out areas where the plastics are present on land and see, as long as the majority of the pixel is composed of polymers. If this is not the case, the B8/B12 difference cannot map out plastics, which was shown in Thilafushi landfill composed of diverse material. More fieldwork and experiments using remote sensing data with ground-truthing is needed to test large areas covered with diverse litter mixed with organic material.

8. Recommendations and future work

Following from the findings of the project, these are the recommendations for the future work:

1. Test other study areas where plastic objects area static (we know that particular pixels are covered in polymers without ground-truthing) or conduct fieldwork and look at the spectral signature graphs of these objects.

2. Maximum likelihood classification (or other image classification method-object oriented) of WV3 for Mytilene case study. Compare the results to Sentinel 2 data for 06/07/2018 to see how higher spatial resolution can improve image classification.

3. Explore SWIR wavebands from WV3- in particular SWIR 1 which corresponds to 1215 nm and SWIR 4- 1730 nm that were used by Garaba and Dierssen (2018) and Martinez-Vincent et al. (2019) to successfully identify polymers.

9. References

Asner, G. (2016) Workshop on mission concepts for marine debris sensing, January 19–21, 2016, east-west center of the university of Hawaii at Manoa, Honolulu, Hawaii, available online: http://iprc.soest.hawaii.edu/NASA_WS_MD2016/pdf/Asner2016

Azzarello MY, Van-Vleet ES (1987) Marine birds and plastic pollution in *Marine Ecological Progress Series,* Vol. 37, 295–303

Boerger CM, Lattin GL, Moore SL, Moore CJ (2010) Plastic ingestion by planktivorous fishes in the North Pacific Central Gyre in *Marine Pollution Bulletin*, 60(12):2275–2278

BBC (2011) online website accessed 30/04/2019, available from https://www.bbc.co.uk/news/world-asia-16072020

Choy CA, Drazen JC (2013) Plastic for dinner? Observations of frequent debris ingestion by pelagic predatory fishes from the central North Pacific in *Marine Ecological Progress Series* Vol.485, 155–163

Cózar, A., Echebarría, F., González-Gordillo, J.I., Irigoien, X, Úbeda, B., Hernández-León, S., Palma, T.A., García-de-Lomas, J., Ruiz, A., Fernández-de-Puelles, M.L. and Duarte, M. (2014) Plastic debris in the open ocean in *PNAS,* Vol. 11 (28), 10239-10244

de Stephanis R, Giménez J, Carpinelli E, Gutierrez-Exposito C, Cañadas A (2013) As main meal for sperm whales: Plastics debris in *Marine Pollution Bulletin* 69(1–2):206–214

EU Commission (2018) A European Strategy for Plastic in a Circular Economy, online version available from https://eur-lex.europa.eu/legal-content/EN/TXT/?qid=1516265440535&uri=COM:2018:28:FIN

Eden (2019) online website available from: https://www.edenproject.com/eden-story/behind-the-scenes/architecture-at-eden

Galgani, Hanke and Maes (2015) Global Distribution, Composition and Abundance of Marine Litter, Chapter 2 in *Marine Anthropogenic Litter*

Garaba, P., S. and Dierssen, H.M. (2018) An airborne remote sensing case study of synthetic hydrocarbon detection using short wave infrared absorption features identified from marine harvested macro- and mictorplastics in *Remote Sensing of Environment*, 2015, 224-235

Lebreton, L.C.M., Greer, S.D., and Borrero, J.C. (2012) Numerical modelling of floating debris in the world's oceans in *Marine Pollution Bulletin*, Vol 64 (3), 653-661

Lebreton, L., Slat, B., Ferrari, F., Sainte-Rose, B., Aitken, J., Marthouse, R., Hajbane, S., Cunsolo, S., Schwarz, A., Levivier, A., Noble, K., Debeljak, P., Maral, H., Schoeneich-Argent, R., Brambini, R. and Reisser, J. (2018), Evidence that the Great Pacific Garbage Patch is rapidly accumulating plastic, in *JO - Scientific Reports*

Maes, T. (2017) ICES News- Marine litter and monitoring, online version available from http://ices.dk/news-and-events/news archive/news/Pages/FEATURE%20ARTICLE%20%E2%80%93%20Marine%20litter%20and%20monitoring.aspx

Marine Remote Sensing Group (2019) online website available from: https://mrsg.aegean.gr/?content=&nav=55

Martinez-Vincent, V., Mata, A., Biermann, L., Clark, J., Lindeque, P. and Corradi, P. (2019) Optical methods for marine litter detection (OPTIMAL): from user requirements to roadmap design for marine plastic detection system, Atlantic From Space Workshop, 23-25th January 2019, Southampton UK, available online from https://www.dropbox.com/sh/hza9d8d6hn8zk6l/AADA5Br3Rf4bp9viLQ2DeijZa?dl=0

Maximenko, N., Hafner, J. and Niiler, P. (2012) Pathways of marine debris derived from trajectories of Lagrangian drifters in *Marine Pollution Bulletin* ,65 (1–3):51–62

Maximenko, N., Arvesen, J., Asner, G., Carlton, J., Castrence, M., Centurioni, L., Chao, Y., Chapman, J., Chirayath, V., Corradi, P., Crowley, M., Dierssen, H.M., Dohan, K., Eriksen, M., Galgani, F., Garaba, S.P., Goni, G., Griffin, D., Hafner, J., Hardesty, D., Isobe, A., Jacobs, G., Kamachi, M., Kataoka, T., Kubota, M., Law, K.L., Lebreton, L.,Leslie, H.A., Lumpkin, R., Mace, T.H., Mallos, N., McGillivary, P.A., Moller, D., Morrow, R., Moy, K.V., Murray, C.C., Potemra, J., Richardson, P., Robberson, B., Thompson, R., van Sebille, E., Woodring, D. (2016) Remote Sensing of Marine Debris to Study Dynamics, Balances and Trends in *White Paper from Workshop on Mission Concepts for Marine Debris Sensing,* pp. 22 Submitted to Decadal Survey for Earth Science and Applications from Space

Moller, D., Chao, Y., Maximenko, N. (2016) Remote sensing of marine debris in *EEE International Geoscience and Remote Sensing Symposium (IGARSS)* http://dx.doi.org/10.1109/IGARSS.2016.7731005

Murphy, L., G., Peters, S., Sebille, van E., James, N.A. and Gibb, S. (2018) Concept for a hyperspectral remote sensing algorithm for floating marine macro plastics in *Marine Pollution Bulletin*, 126, 255-262

Teuten, E., L., Saquing, J.M., Knappe, D.R.U., Barlaz, M.A., Jonsson, S., Björn, A., Rowland, S.J., Thompson, R.C., Galloway, T.S., Yamashita, R., Ochi, D., Watanuki, Y., Moore, Ch., Hung Viet, P., Tana, T.S., Prudente, M., Boonyatumanond, R., Zakaria, M., P., Akkhavong, K., Ogata, Y., Hirai, H., Iwasa, S., Mizukawa, K., Hagino, Y., Imamura, A., Saha, M. and Takada, H. (2009) Transport and release of chemicals from plastics to the environmentand to wildlife. Philos Trans R Soc Lond B Biol Sci 364(1526):2027–2045

Topouzelis, K. and Papakonstantinou, A. (2019) Plastic litter detection from space: current knowledge and lessons learned from the Plastic Litter Project 2018, Atlantic From Space Workshop, 23-25th January 2019, Southampton UK, available online from
https://www.dropbox.com/sh/hza9d8d6hn8zk6l/AADA5Br3Rf4bp9viLQ2DeijZa?dl=0

10. Appendix

Appendix 1:

Eden study area									
Cover type	Urban			Vegetation			Water		
Band	B8	B9	B12	B8	B9	B12	B8	B9	B12
Min	0.008	0.091	0.099	0.202	0.219	0.06	0.008	0.091	0.014
Max	0.595	0.472	0.23	0.455	0.472	0.106	0.075	0.181	0.06
Mean	0.275	0.28	0.182	0.34	0.367	0.075	0.03	0.153	0.024
STD	0.143	0.089	0.04	0.089	0.086	0.015	0.019	0.03	0.12
Coefficient of variation	0.52	0.317	0.229	0.262	0.234	0.199	0.625	0.197	0.522
Eden study area									
Cover type	Agriculture			Dome 1			Dome 2		
Band	B8	B9	B12	**B8**	B9	**B12**	**B8**	B9	**B12**
Min	0.148	0.155	0.052	**0.314**	0.238	**0.152**	**0.282**	0.248	**0.149**
Max	0.475	0.469	0.233	**0.595**	0.328	**0.307**	**0.551**	0.332	**0.233**
Mean	0.29	0.306	0.137	**0.393**	0.295	**0.193**	**0.352**	0.285	**0.177**
STD	0.114	0.11	0.067	**0.092**	0.029	**0.047**	**0.083**	0.0285	**0.025**
Coefficient of variation	0.393	0.36	0.492	**0.236**	0.099	**0.248**	**0.237**	0.1	**0.144**

Appendix 2:

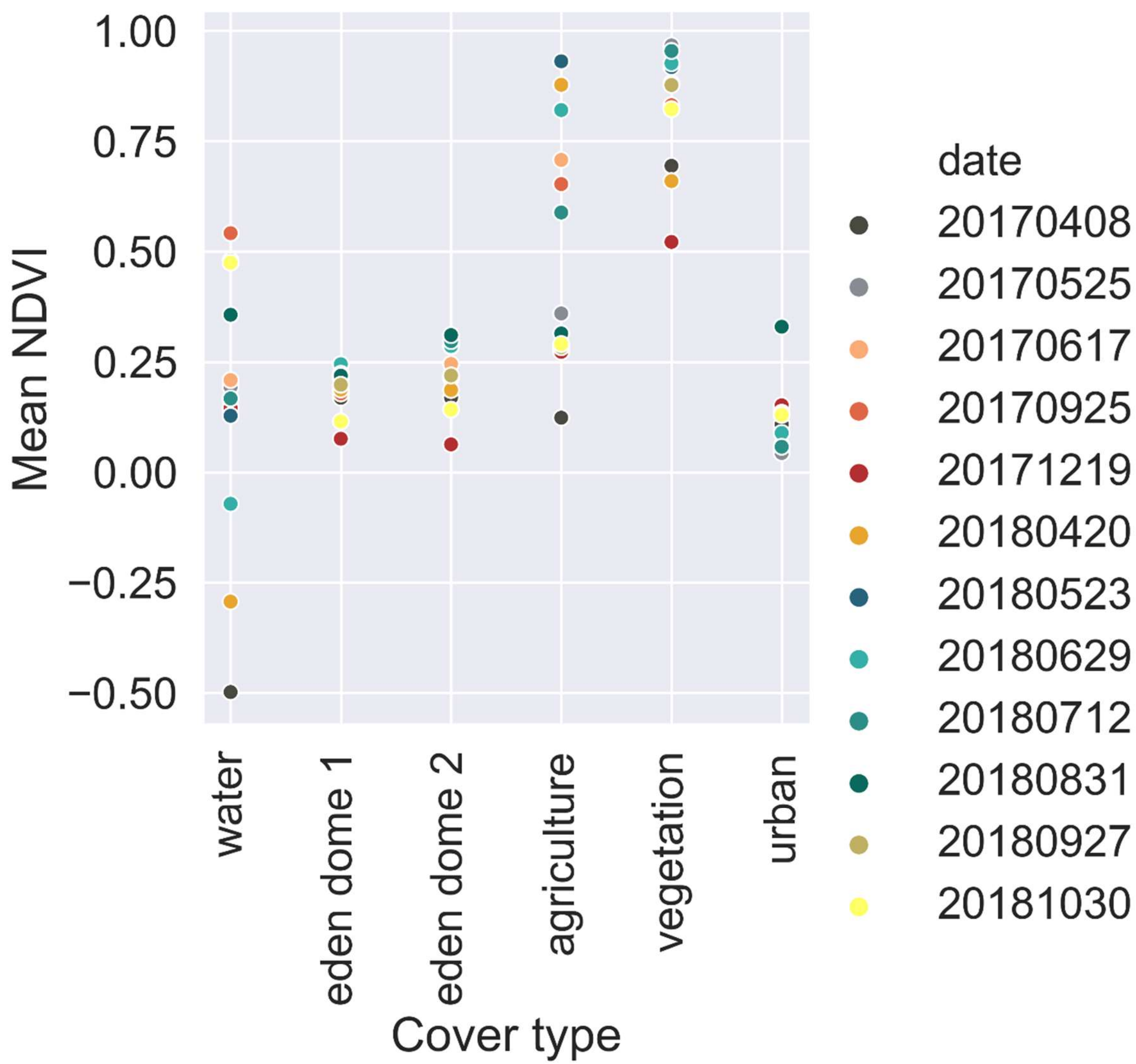
1.00
0.75
0.50
0.25
0.00
−0.25
−0.50
Mean NDVI
water
eden dome 1
eden dome 2
agriculture
vegetation
urban
Cover type
date
20170408
20170525
20170617
20170925
20171219
20180420
20180523
20180629
20180712
20180831
20180927
20181030